JOURNAL OF APPLIED ELECTROCHEMISTRY 15 (1985) 527–536

*Mass diffusion-controlled bubble behaviour in boiling and electrolysis and effect of bubbles on ohmic resistance**

S. J. D. VAN STRALEN, W. M. SLUYTER

Eindhoven University of Technology, Department of Physics, PO Box 513, 5600 MB Eindhoven, The Netherlands

Received 16 December 1984

A survey is given of theoretical asymptotic bubble behaviour which is governed by heat or/and mass diffusion towards the bubble boundary. A model has been developed to describe the effect of turbulent forced flow on both bubble behaviour and ohmic resistance. A comparison with experimental results is also made.

Nomenclature

a	liquid thermal diffusivity ($m^2\ s^{-1}$)
B	width of electrode (m)
c	liquid specific heat at constant pressure ($J\,kg^{-1}\,K^{-1}$)
ΔC_0	initial supersaturation of dissolved gas at the bubble wall ($kg\,m^{-3}$)
d	bubble density at electrode surface (m^{-2})
D	diffusion coefficient of dissolved gas ($m^2\,s^{-1}$)
D_h	$-4S/Z$, hydraulic diameter, with S being the cross-sectional area of the flow and Z being the wetted perimeter (m)
e	base of natural logarithms, 2.718...
f	local gas fraction
F	Faraday constant ($C\,kmol^{-1}$)
G	evaporated mass diffusion fraction
h	height from bottom of the electrode (m)
h_w	total heat transfer coefficient for electrode surface ($J\,s^{-1}\,m^{-2}K^{-1}$)
$h_{w,conv}$	convective heat transfer coefficient for electrode surface ($J\,s^{-1}\,m^{-2}K^{-1}$)
H	total height of electrode (m)
i	electric current density ($A\,m^{-2}$)
j, j^*	number
Ja	modified Jakob number, $\Delta C_0/\rho_2$
$\mathscr{L}$	enthalpy of evaportion ($J\,kg^{-1}$)
m	density of activated nuclei generating bubbles at electrode surface (m^{-2})
n	product of valency and number of equal ions forming one molecule; for hydrogen $n = 2$, for oxygen $n = 4$
p	pressure ($N\,m^{-2}$)
Δp	excess pressure ($N\,m^{-2}$)
$\hat{R}$	gas constant ($J\,kmol^{-1}\,K^{-1}$)

* Paper presented at the International Meeting on Electrolytic Bubbles organized by the Electrochemical Technology Group of the Society of Chemical Industry, and held at Imperial College, London, 13–14 September 1984.

0021–891X/85 $03.00 + .12

R_1 bubble departure radius (m)
R_0 equilibrium bubble radius (m)
$\Delta R/R$ relative increase of ohmic resistance due to bubbles, ΔR, in comparison to corresponding value, R, for pure electrolyte
Re Reynolds number, vD_h/ν
Sc Schmidt number, ν/D
Sh Sherwood number $D_h/\bar{\delta}_m$
t time (s)
T absolute temperature (K)
ΔT increase in temperature of liquid at bubble boundary with respect to original liquid in binary mixture (K)
v solution flow velocity ($m\,s^{-1}$)
x mass fraction of more volatile component in liquid at bubble boundary in binary mixture
x_0 mass fraction of more volatile component in original liquid in binary mixture
y mass fraction of more volatile component in vapour of binary mixture
α contact angle
δ local thickness of one phase velocity boundary layer (m)
δ_m local thickness of corresponding mass diffusion layer (m)
δ^* local thickness of two-phase velocity boundary layer (m)
θ_0 initial liquid superheating (K)
κ constant in Henry's law ($m^2\,s^{-2}$)
ν liquid kinematic viscosity ($m^2\,s^{-1}$)
ν^* bubble frequency at nucleus (s^{-1})
ρ_1 liquid mass density ($kg\,m^{-3}$)
ρ_2 gas/vapour mass density ($kg\,m^{-3}$)
σ surface tension ($N\,m^{-1}$)

1. Bubble behaviour

A survey on bubble behaviour has been presented by Van Stralen and Cole [1] concerning both vapour bubbles generated during nucleate boiling and gas bubbles evolved during electrolysis.

In general, initial bubble growth is determined by liquid inertia. During boiling, especially at atmospheric and elevated pressures, the initial superheating of the vapour bubble boundary decreases due to evaporation and advanced bubble growth is governed by heat diffusion. The slow growth of gas bubbles evolved during (alkaline) water electrolysis is completely determined by mass diffusion of the gas in the liquid.

In the most general case of boiling binary (or multicomponent) systems, advanced bubble growth is determined by combined heat and mass diffusion. This results in a remarkable slowing down of both bubble growth rate and departure size at a certain low concentration of the more volatile component; this concentration depends on vapour–liquid equilibrium data of the system.

The practical use of investigating bubble behaviour during boiling is to derive dimensionless correlations for the (maximum) heat flux. For electrolysis, the aim is to optimize the energy efficiency, which depends on bubble behaviour. For the mechanism, of boiling heat transfer, reference is made to Van Stralen's 'relaxation microlayer' model for the nucleate boiling heat flux [1]. An analogous model for mass transfer during electrolysis has been developed by Janssen and Van Stralen [2]. The theoretical treatment of bubble growth is presented in sections 2–5.

2. Growth of free vapour bubbles in superheated pure liquids

2.1. *Initial growth*

The 'equilibrium' value of the bubble radius in a uniformly superheated liquid is given by:

$$R_0 = \frac{2\sigma}{\Delta p} \tag{1}$$

Assuming thermodynamic equilibrium, the required excess pressure is derived from the Clapeyron equation:

$$\Delta p = \frac{\rho_2 \mathscr{L}}{T}\theta_0 \tag{2}$$

The initial mode of growth is inertia controlled, i.e. the bubble is blown up according to:

$$R(t) \approx \left(\frac{2\Delta p}{3\rho_1}\right)^{1/2} t = \left(\frac{2\rho_2 \mathscr{L}}{3\rho_1 T}\right)^{1/2} t \sim (p\theta_0)^{1/2}\, t \tag{3}$$

2.2. *Transitional growth*

$\theta_R(t)$ decreases from the original value, θ_0, to zero due to evaporation (Fig. 1).

2.3. *Asymptotic growth*

The temperature at the bubble boundary has dropped to the saturation value at ambient pressure, p. Asymptotic bubble growth is heat diffusion controlled i.e. governed by the heat flow towards the bubble boundary:

$$R(t) \cong \left(\frac{12}{\pi}\right)^{1/2} Ja(at)^{1/2} \sim (\theta_0/p)t^{1/2} \qquad \text{as } Ja \gg \frac{\pi}{6} \tag{4}$$

$$R(t) \cong (2Ja)^{1/2}(at)^{1/2} \sim (\theta_0/p)^{1/2} t^{1/2} \qquad \text{as } Ja \ll \frac{\pi}{6} \tag{5}$$

The Jakob number $Ja = \rho_1 c\theta_0/\rho_2 \mathscr{L}$. In general, Equation 4 applies to boiling, both equations apply to electrolysis. The transitions, case 2.2, from Equation 4 to Equation 5 can be given by analytical expressions, cf. Equation 7.

3. Growth of (electrolytic) gas bubbles

Equation 2 is replaced by Henry's law:

$$\Delta p = \kappa \Delta C_0$$

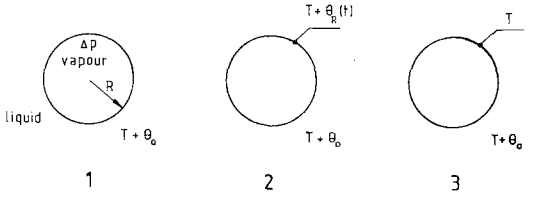

Fig. 1. Decrease of superheating, $\theta_R(t)$, at bubble boundary from θ_0 to zero during bubble growth: (1) initial bubble growth is inertia controlled; (2) transitional mode of growth; (3) asymptotic growth is diffusion controlled.

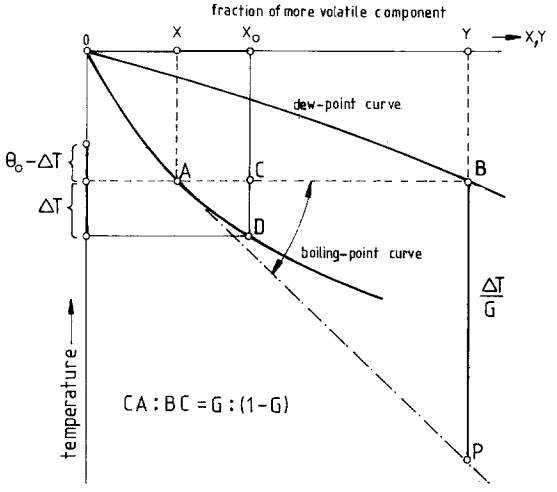

Fig. 2. Equilibrium diagram at constant pressure for a binary system with a more volatile component. Asymptotic bubble growth is combined heat and mass diffusion controlled, i.e. θ_0 is replaced by $\theta_0 - \Delta T(x_0)$; this results in a slowing down of bubble growth at a certain low concentration of the more volatile component. $G = (x_0 - x)(y - x) \rightarrow BP = CD(BA/CA) = \Delta T/G$. $\Delta T/G$ depends on x_0, but is independent of both θ_0 and G.

Here, the Jakob number $Ja = \rho_1 x_0 p_2 = \Delta C_0/\rho_2$. Bubble growth is completely mass diffusion controlled; this is due to the low value of the mass diffusivity, D, resulting in a very rapidly diminishing supersaturation at the bubble wall.

Due to the analogy between heat and mass diffusion, one has to replace a by D in Equations 4 and 5.

4. Growth of free bubbles in superheated binary systems with a more volatile component

Combined heat and analogous mass diffusion results in a slowing down of bubble growth at a certain low concentration of the more volatile component [1] (see Fig. 2):

$$Ja = \rho_1 c(\theta_0 - \Delta T)/\rho_2 \mathscr{L} = \frac{\rho_1 c \theta_0}{\rho_2 \mathscr{L}} \left[1 + \left(\frac{a}{D}\right)^{1/2} \frac{c}{\mathscr{L}} \frac{\Delta T}{G}\right]^{-1} \leqslant \rho_1 c \theta_0/\rho_2 \mathscr{L} \qquad (6)$$

e.g. In water-2-butanone $\theta_0 - \Delta T = 0.25\,\theta_0$ at 4 wt% 2-butanone. Also, bubble coalescence is prevented in 'positive' systems due to the Marangoni effect.

5. Gas bubbles at electrodes

The growth rate of these bubbles is very small due to the low values of both Ja and D. The bubbles are 'cavity' bubbles [3], i.e. their base is limited to the originating cavity at the electrode surface and does not spread along the surface. The bubbles are 'nearly' spherical due to the small contact ('wetting') angle α (Fig. 3).

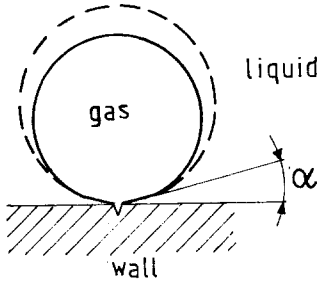

Fig. 3. Growth of a 'cavity' bubble.

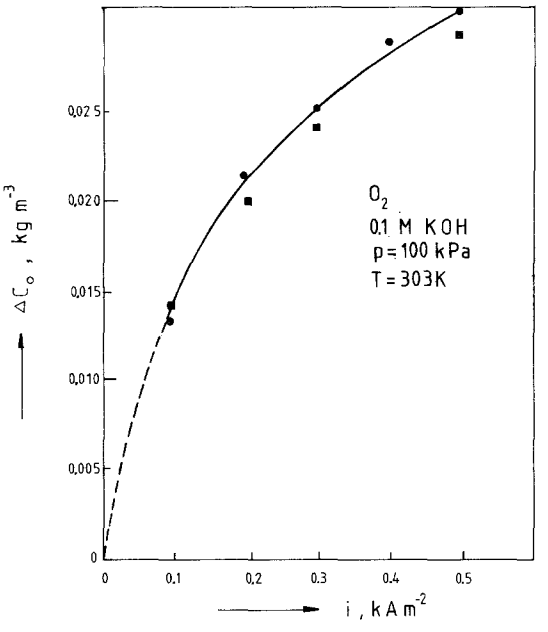

Fig. 4. Alkaline water electrolysis. Averge supersaturation of oxygen at anode surface in dependence on current density [4].

The (unknown) supersaturation, ΔC_0, can be derived from experiments using the following transitional growth equation:

$$R(t) \cong \left(\frac{3}{\pi}\right)^{1/2} Ja\left[1 + \left(1 + \frac{2\pi}{3Ja}\right)^{1/2}\right](Dt)^{1/2} \tag{7}$$

Equation 6 is a generalization, which reduces to the limiting cases, i.e. to Equation 4

as $Ja \to \infty$ and to Equation 5

as $Ja \to 0$.

The theory has been shown to be in agreement with a large number of (high speed cinematographic) experiments. To calculate ΔC_0, the reverse order is taken. Results are shown in Fig. 4, [4].

6. Hydrogen Programme

The experimental part of the hydrogen programme on alkaline water electrolysis carried out by our working group 'Electrolytic gas evolution', a part of which has been supported by the European Communities, includes research on evolved gas bubbles, on their size and spatial distributions, on the local gas fraction and on the relative increase of the electric resistance. In general, the following parameters are varied: pressure, temperature, current density, solution concentration and flow velocity, nature of gas evolved, and electrode material and configuration. A theoretical model for the very important case of forced two-phase flow is given in Section 7.

7. Effect of bubbles on ohmic resistance

The theoretical part of the programme deals with the derivation of a dimensionless correlation for the energy efficiency. A model is proposed here, which is based on an extension of one-phase flow models to corresponding two-phase situations. During two-phase flow, the velocity boundary layer at the electrode is blown up by the bubbles, which are small in comparison to the local thickness, $\delta(h)$, of the velocity boundary layer; this follows from the small values of the Jakob number [1].

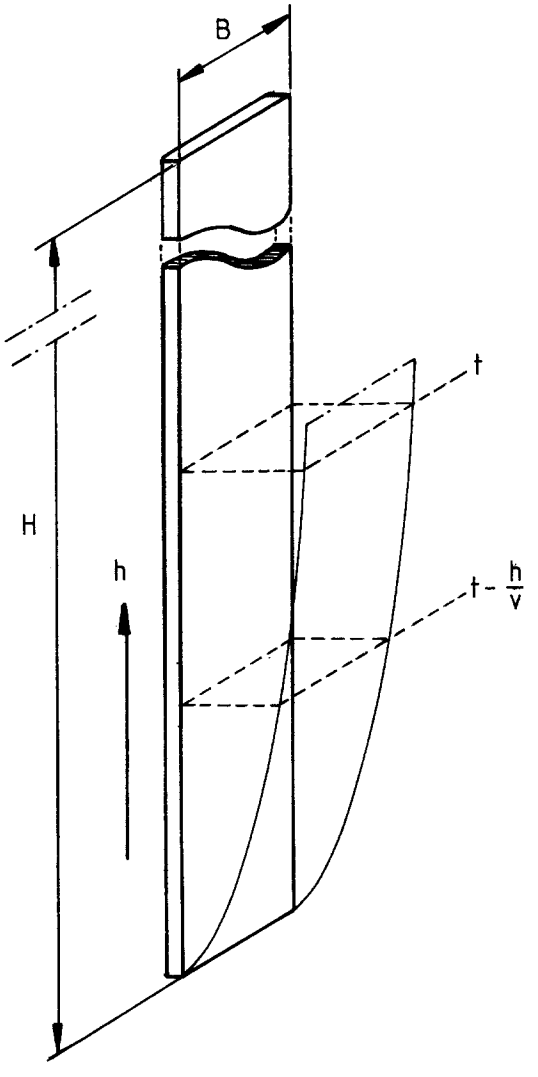

Fig. 5. Upward forced flow along a vertical flat electrode. The thickness of the velocity boundary layer increases with increasing height, h.

At height h of the electrode with upward flowing solution, the local gas fraction (Fig. 5) is given by:

$$f(h) = \left[m\left(\frac{4\pi}{3} R_1^3 v^*\right)\right] \frac{h}{v\delta(h)} \tag{8}$$

Inserting Faraday's law,

$$m\left(\frac{4\pi}{3} R_1^3\right) v^* = \frac{\hat{R}T}{npF}\, i \tag{9}$$

yields,

$$f(h) = \frac{\hat{R}T}{npF} \frac{h}{v\delta(h)} i \tag{10}$$

For hydrogen, $n = 2$; for oxygen $n = 4$.

Similarly to the case of turbulent heat transfer, one can use the following dimensionless correlation as an approximation for the overall one-phase mass transfer: $Sh = 0.023\, Re^{0.8} Sc^{0.4}$, where the Sherwood number $Sh = D_h/\bar{\delta}_m$ and the Schmidt number $Sc = \nu/D$.

As $\bar{\delta} = Sc^{0.4}\bar{\delta}_m$, one has;

$$\bar{\delta}^{-1} = 0.023\, D_h^{-0.2} \nu^{-0.8} v^{0.8} \tag{11}$$

Assuming $\delta(h) \sim h^j$, $\delta(h)/\bar{\delta} = (j+1)(h/H)^j$, results in,

$$\frac{\Delta R}{R} = \frac{3}{2} f = 0.035 \frac{\hat{R}T}{npF} \frac{H^j}{j+1} D_h^{-0.2} \nu^{-0.8} (i h^{1-j} v^{-0.2}) \tag{12}$$

Here, the Maxwell or Bruggeman equations have been applied for $f \ll 1$; practically, the range of validity extends to higher values of f.

Actually, in two-phase flow, δ has to be replaced by $\delta^* = \delta/(1-f)$. The bubbles are assumed to ascend within the velocity boundary layer at the electrode, and the slip ratio equals one. Obviously, $\delta^* \to \infty$ as $f \to 1$; actually, the thickness of the two-phase velocity boundary layer is limited by the hydraulic diameter, D_h, of the cell: $\delta^* \leqslant \frac{1}{2} D_h$. For *laminar* flow, $j = 0.5$, Equation 12 results in:

$$\frac{\Delta R}{R} \sim \frac{h^{0.5}}{v^{0.2}} i \tag{13}$$

Assuming a linear velocity profile in the direction perpendicular to the electrode surface, and taking $j = 0.8$, the case of *turbulent* flow, Equation 12 yields, after introduction of δ^*:

$$\frac{\Delta R}{R} = 1.50 \left[68.2 \frac{npF}{\hat{R}T} \nu^{0.8} D_h^{0.2} H^{-0.8} \left(\frac{v}{h} \right)^{0.2} i^{-1} + 1 \right]^{-1} \tag{14}$$

The dependence of $\Delta R/R$ on flow velocity, on relative height, h/H, in the channel and on current density, are predicted explicitly. The relation $\Delta R/R \sim v^{-0.2}$ is in agreement with experimental results; the dependence on height is investigated by Bongenaar [5, 6]. A modified version of the proposed model has been given by Sillen [7]. Bongenaar [5, 6] found experimentally, that $\Delta R/R \sim (h^{0.3}/v^{0.2}) i^{j^*}$, with $j^*(i) \leqslant 1$.

8. Numerical example

Alkaline water electrolysis (1 M KOH) at $p = 1$ bar and $T = 303$ K, plate electrode (20×500 mm^2) in a cell with cross-sectional area of 20×10 mm^2 (hydraulic diameter $D_h = 13$ mm) and height of the electrode = 0.50 m. Table 1 shows the values of $h = 0.25$ m, calculated by Thommassen [8] from Equation 14.

It may be noticed, that values $j^* < 1$ are apparently due to the bubble behaviour: $i \sim m R_1^3 \nu^*$, cf. Equation 9. At increasing current density, i: $m(i)$ increases and $R_1(i)$ decreases (Fig. 7), i.e. $\Delta C_0(i)$ increases (cf. Fig. 4), but $t_1 = 1/\nu^*$ decreases, thus the bubble frequency ν^* increases; ν^* is also increased by bubble coalescence, which causes departure. The relation $t_1 = 1/\nu^*$ is based on a zero waiting time. Actually, the right hand side of Equation 9 has to be multiplied by an experimentally derived factor of 0.55, a value independent of both i and v [7], i.e. 55% is transferred to adhering bubbles; the remaining 45% to released bubbles.

Table 1. Values calculated by Thommassen from Equation 14.

i (kA m^{-2})	v (m s^{-1})	δ (mm)	$\delta/(1-f)$ (mm)		f		$\Delta R/R$	
			H_2	O_2	H_2	O_2	H_2	O_2
1.8	0.30	1.21	1.53	1.37	0.21	0.12	1.41	1.21
1.8	0.75	0.58	0.71	0.64	0.18	0.10	1.35	1.17
5.5	0.30	1.21	2.20	1.70	0.45	0.29	2.45	1.67
5.5	0.75	0.58	0.98	0.78	0.41	0.26	2.20	1.56
9.1	0.30	1.21	2.87	2.05	0.58	0.41	3.67	2.20
9.1	0.75	0.58	1.23	0.91	0.53	0.36	3.10	1.95

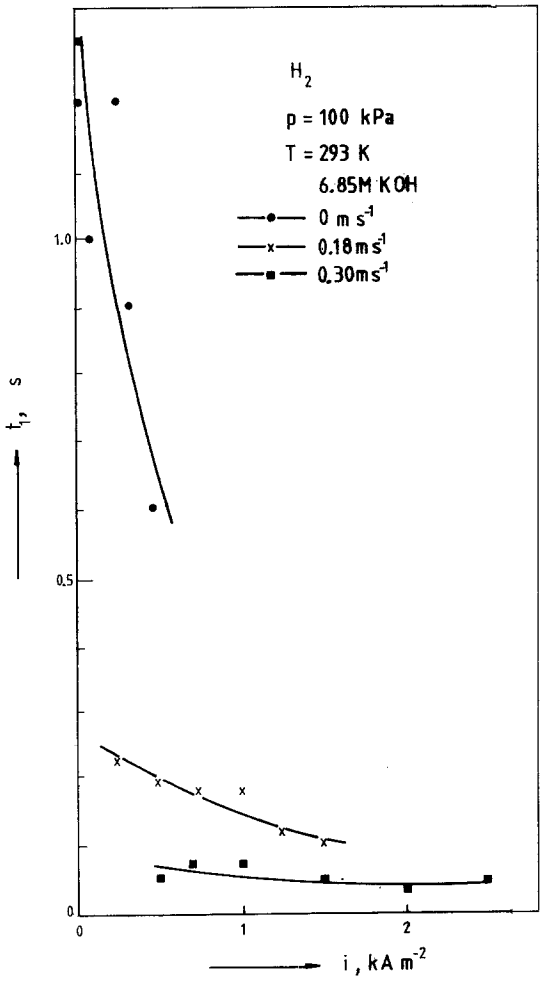

Fig. 6. Alkaline water electrolysis. Dependence of average hydrogen bubble departure time on current density at forced convection ($v = 0.18\ \mathrm{m\ s^{-1}}$ and $v = 0.30\ \mathrm{m\ s^{-1}}$) in comparison to free convection ($v = 0$), cf. [7]. $\bar{t}_1$ decreases both at increasing i and v. This is in agreement with Van Stralen's 'relaxation microlayer' model [1], according to which $t_1 \sim h_{\mathrm{w,co}}^{-2}$.

This is in quantitative agreement with Van Stralen's 'relaxation microlayer' model [1] for heat and mass transfer in boiling and electrolysis, respectively:

$$h_{\mathrm{w}} = \left(1 + \frac{32}{3\pi e}\right) h_{\mathrm{w,conv}} = 2.24\, h_{\mathrm{w,conv}} \tag{15}$$

The additional factor denotes the promoting effect of bubbles on two-phase flow transport. The effect of the adhering bubbles amounts to $1.24/2.24 = 0.55$. This expression is based on a bubble density $m = 1/\pi R_1^2$; the region of influence of a bubble equals $4\pi R_1^2/3e = 1.54\, R_1^2 = 0.49(\pi R_1^2)$. Bubble coalescence promotes the maximal gas production rate and decreases the degree of screening of the electrode.

Figs. 6–8 show experimental results on the effect of i obtained by Sillen [7] for forced convection in comparison to free convection ($v = 0$): Fig. 6 shows the average bubble departure time, $\bar{t}_1$, Figs. 7 and 8 the average bubble density, $\bar{d}$, and bubble radius, $\bar{R}$, at the electrode surface, for hydrogen and oxygen, respectively. Discontinuities in the curves are caused by bubble coalescence. Optically transparent gold or nickel-plated glass electrodes were used in combination with high speed cinematography.

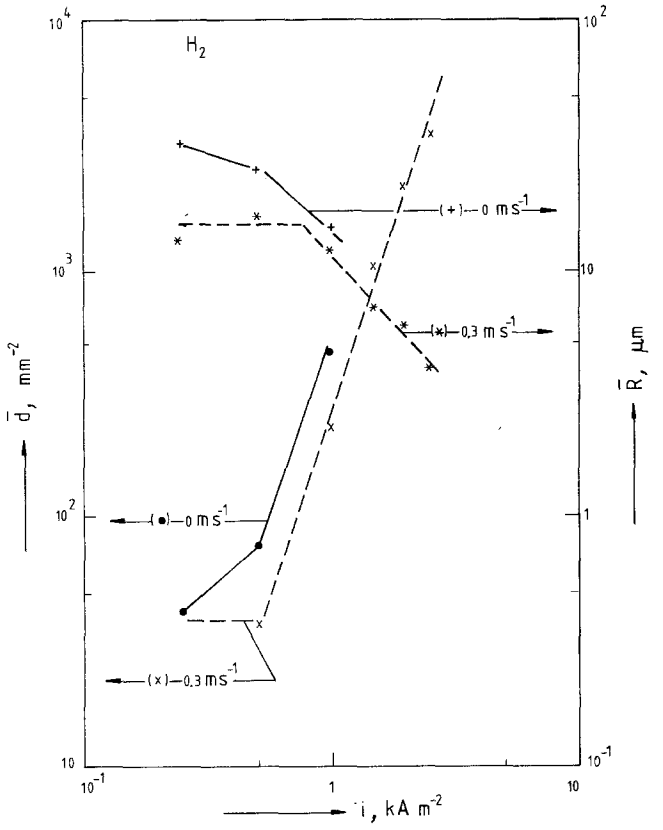

Fig. 7. Alkaline water electrolysis. Average hydrogen bubble density, $\bar{d}$, and bubble radius, $\bar{R}$, at cathode surface in dependence on current density [7] at forced convection ($v = 0.3\ \mathrm{m\,s^{-1}}$) in comparison to free convection ($v = 0$). $\bar{d}$ increases and $\bar{R}$ decreases at increasing i. Both $\bar{d}$ and $\bar{R}$ decrease at increasing v. Discontinuities in the curves at a certain value of i are due to bubble coalescence.

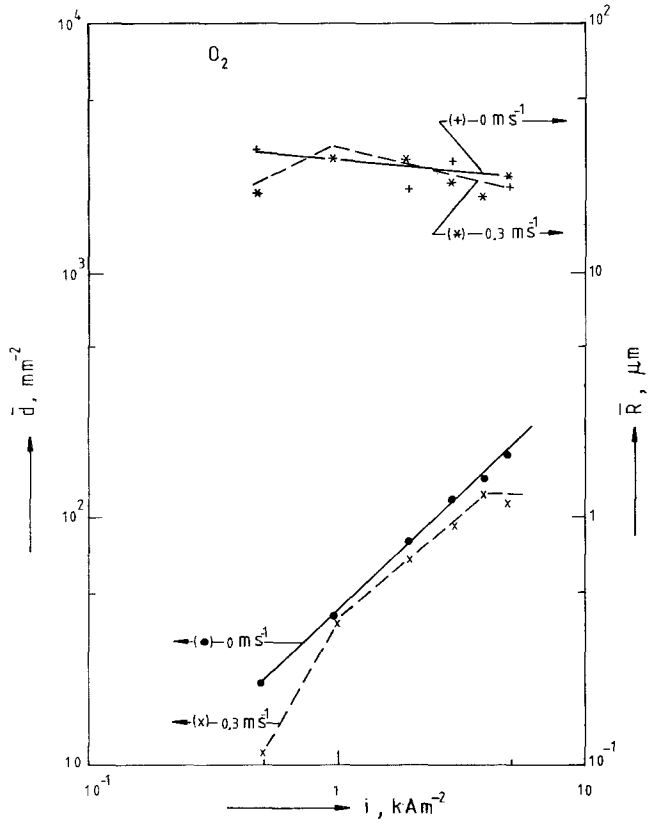

Fig. 8. Alkaline water electrolysis. Average oxygen bubble density, $\bar{d}$, and bubble radius, $\bar{R}$, at anode surface in dependence on current density [7] at forced convection ($v = 0.3\ \mathrm{m\,s^{-1}}$) in comparison to free convection ($v = 0$), cf. Fig. 7 for hydrogen. $\bar{d}$ increases at increasing i. The effects of both i and v on $\bar{R}$ are small.

References

[1] S. J. D. van Stralen, R. Cole, 'Boiling Phenomena', Vols. 1 and 2, Hemisphere, Washington/McGraw-Hill, New York (1979).
[2] L. J. J. Janssen and S. J. D. van Stralen, *Electrochim. Acta* **26** (1981) 1011.
[3] P. C. Slooten, PhD Thesis, Eindhoven University of Technology, Eindhoven (1984).
[4] H. M. S. Wedershoven, R. M. de Jonge, C. W. M. P. Sillen and S. J. D. van Stralen, *Int J. Heat Mass Transfer* **25** (1982) 1239.
[5] B. E. Bongenaar-Schlenter, PhD Thesis, Eindhoven University of Technology, Eindhoven (1984).
[6] B. E. Bongenaar-Schlenter, L. J. J. Janssen, S. J. D. van Stralen and E. Barendrecht, *J. Appl. Chem.* **15** (1985) 537.
[7] C. W. M. P. Sillen, PhD Thesis, Eindhoven University of Technology, Eindhoven (1983).
[8] P. J. M. Thommassen, M. Thesis, Eindhoven University of Technology, Eindhoven (1982).